Supplementary Material:

Chemical signatures of surface microheterogeneity on liquid mixtures

Shinichi Enami*[a], Shinnosuke Ishizuka[a] and Agustín J. Colussi*[b]

[a]*National Institute for Environmental Studies, 16-2 Onogawa, Tsukuba 305-8506, Japan*

[b]*Linde Center for Global Environmental Science, California Institute of Technology, Pasadena, California 91125, USA.*

*Authors to whom correspondence should be addressed: S.E. E-mail: enami.shinichi@nies.go.jp. Phone: 81-29-850-2770. A.J.C. E-mail: ajcoluss@caltech.edu. Phone: +1-626-395-6350.

Validation Experiments

1- Detected products are formed in the outermost interfacial layers of liquid microjets.

Evidence supporting this statement was obtained in previous experiments performed in a similar setup, in which microjets of 1 mM hexanoic acid (PCOOH) solutions in 1:1/H_2O:D_2O (initially at pH 7) were exposed to HNO_3(g) or DNO_3(g). The simultaneous detection of hexanoate ($PCOO^-$, m/z = 115), nitrate (m/z = 62), $PCOOH_2^+$ (m/z = 117), $PCOOHD^+$ (m/z = 118) and $PCOOD_2^+$ (m/z = 119) showed that: (1) interfacial layers were immediately acidified upon exposure, (2) the increase of nitrate was accompanied by the decrease of hexanoate, and (3) the distribution of $PCOOH_2^+$ (m/z = 117), $PCOOHD^+$ (m/z = 118) and $PCOOD_2^+$ (m/z = 119) isotopomers depended on whether the liquid microjets were exposed to HNO_3(g) or DNO_3(g).[1] Since the hydrons (H^+ or D^+) delivered by HNO_3(g) or DNO_3(g) were > 10^3 times smaller than those carried by the 50 μL/min H_2O:D_2O (1:1 = vol:vol) microjets, the implication is that these events took place in interfacial layers of ~1 nm thickness.

2- Detected products are formed on the surface of intact liquid microjets rather than on the microdroplets produced by nebulization or in the gas-phase.

This statement is based on experiments in which we compared the formation of products from O_3(g) reaction with β-caryophyllene injected into the reaction chamber of the mass spectrometer in two ways: **(A)** as 1 mM **β-caryophyllene solution** microjets at 100 μL/min, which amounts to the introduction of 1×10^9 β-caryophyllene molecules/s: Figures 1, main text, S5 and S6. **(B)** as 1 L/min of N_2(g) saturated with **β-caryophyllene vapor** (2.5×10^{14} molecules/cm^3) in equilibrium with liquid β-caryophyllene at 298 K, which amounts to the

introduction of 4×10^{15} β-caryophyllene molecules/s (i.e., in large excess over case **A**): Figure S2. Product signals within background noise in case **B** demonstrate the negligible contribution of reactions on microdroplets on in the gas-phase in our experiments.

3- The main role of the applied electric field is to deflect and accelerate the charged microdroplets towards the polarized entrance to the heated capillary interface.

Figure S3 shows that both HH and FC signal intensities strictly increase (correlation coefficient ρ^2 = 0.99) as the square root of the polarizing high voltage. This dependence strongly suggests a kinematic effect on the trajectory of microdroplets rather than an effect on the chemistry.

In Figure S1, note that the microdroplets generated by nebulization are carried along the y-axis by the nebulizer gas at 160 m/s. At this velocity, microdroplets cover the 2 cm separating the tip of the injector from the projection of the entrance to the heated capillary section of the mass spectrometer in τ = 0.125 ms. The application of an electric field is necessary to deflect the microdroplets along to the x-axis towards the entrance. The acceleration *a* imposed on the microdroplets by the electric field is given by equation SE1:

$$a = \left(\frac{charge}{mass}\right) \frac{V}{d} \qquad \text{(SE1)}$$

Where charge (Coulombs) and mass (Kg) are those of microdroplets, V (Volts) is the potential difference between the grounded injector and entrance to capillary interface, and *d* (m) the distance between these two points. Note that the mass of microdroplets is not constant due to solvent evaporation. In contrast, the charge of microdroplets could only change in Coulomb explosions. The applied voltages V

must be such that the x = 10 mm distance is covered by the accelerated droplets in times $t \sim \tau$, equation SE2:

$$x = {}^{1}/_{2}\left(\frac{charge}{mass}\right)\frac{V}{d}\ t^{2} \qquad \text{(SE2)}$$

SE2 shows that $t \propto V^{-1/2}$. The shorter time *t* is, the larger number of microdroplets will be deflected to the polarized capillary interface and the charges they carry detected by the mass spectrometer, i.e., mass spectral signal intensities are expected to increase as $V^{1/2}$ as observed. The stronger $V^{1/2}$ dependence of the HH signals relative to FC signals (Figure S3) can be explained by the fact that the neutral α-hydroxy-hydroperoxides will only bind to chloride after microdroplets are desolvated in the heated capillary solvent. Therefore, less neutral α-hydroxy-hydroperoxides will evaporate and be lost in the chamber at shorter *t* times.

4- Effects of temperature of drying gas on signals

Figure S4 shows that both FC and HH signals increase with drying gas temperature, showing that thermally labile α-hydroxy-hydroperoxides are sufficiently stable to be detected under present conditions. Incipient decomposition seems to begin only above 300 °C.

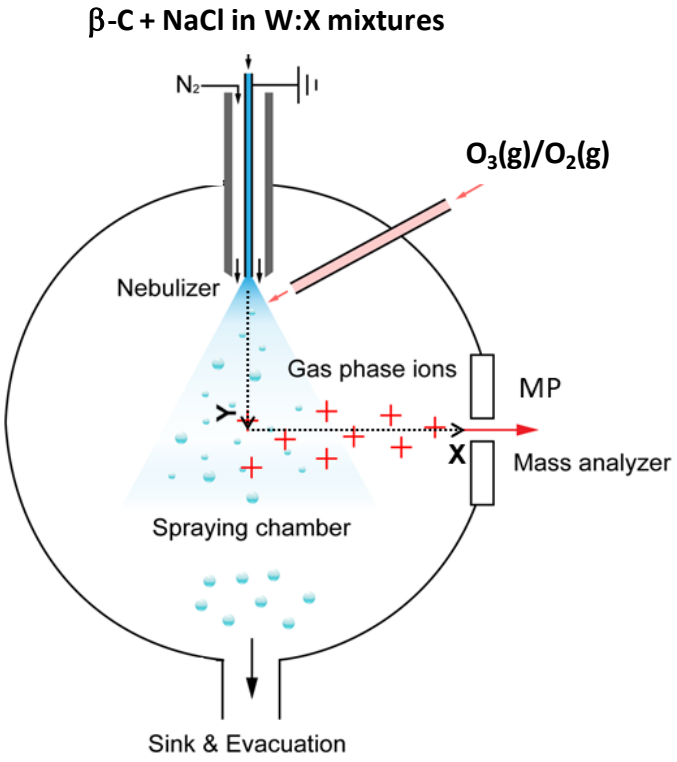

Figure S1 –Schematic diagram of the experimental setup. MP stands for metal plate.

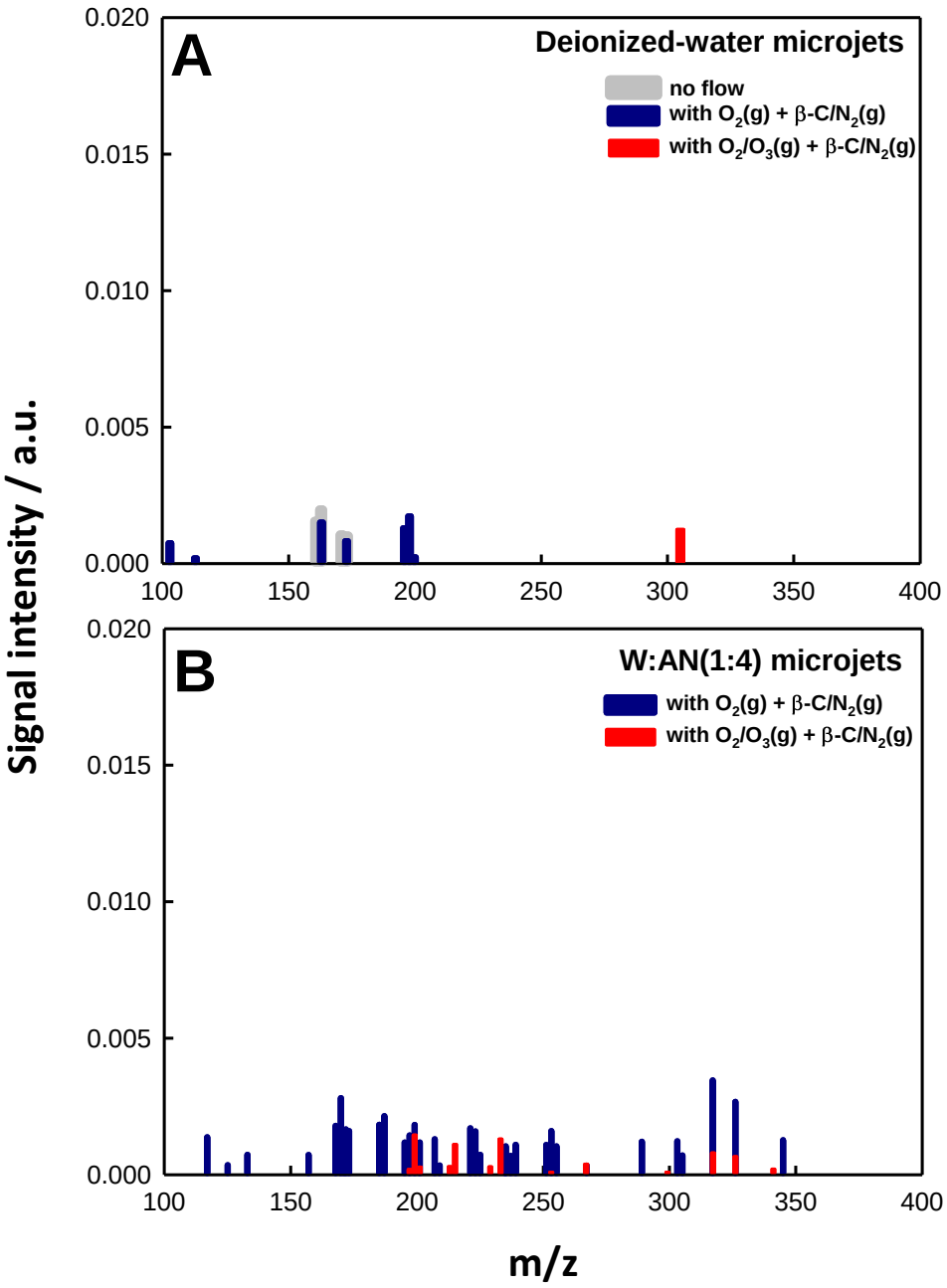

Figure S2. Negative ion mass spectra of the interfacial layers of **A:** deionized-water, **B**: W:AN (x_w = 0.42) liquid microjets. **Gray:** no gas flow. **Dark blue:** exposed to 1 L/min O_2(g) + 1 L/min β-C/N_2(g). **Red:** exposed to 1 L/min O_2/O_3(g) + 1 L/min β-C/N_2(g). Compare with Figures 1 (main text), S5 and S6. Products ion signal intensities are within the background noise. See text on Validation Experiments for further details.

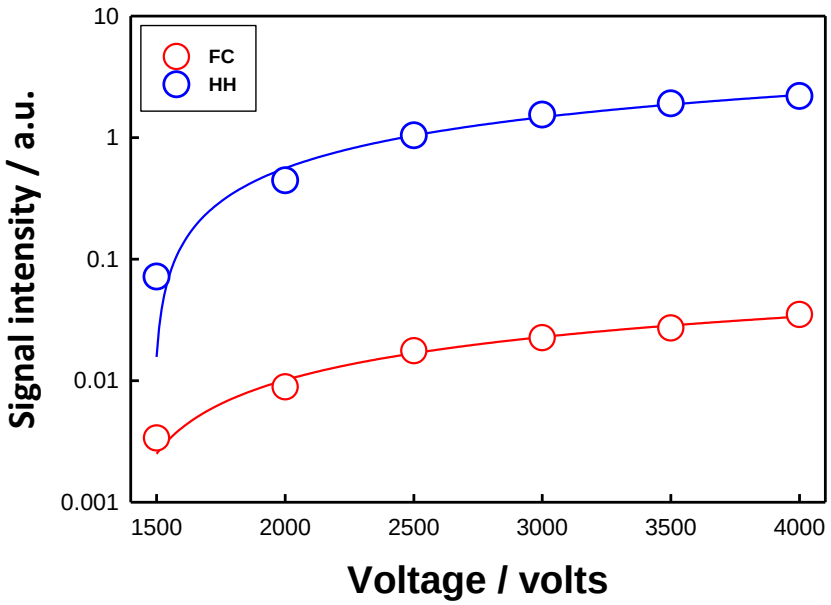

Figure S3 –Mass spectral signal intensities at m/z 251 (FC, red) and 305;307 (HH, blue) from [1 mM β-C + 0.2 mM NaCl] in a x_w = 0.42 W:AN solution microjet exposed to O_3(g) [$E(O_3)$ = 8.1 x 10^{10} molecules cm^{-3} s] as a function of capillary voltage (volts). Lines correspond to Signal intensity = a + b $V^{1/2}$ regressions (ρ^2 = 0.99).

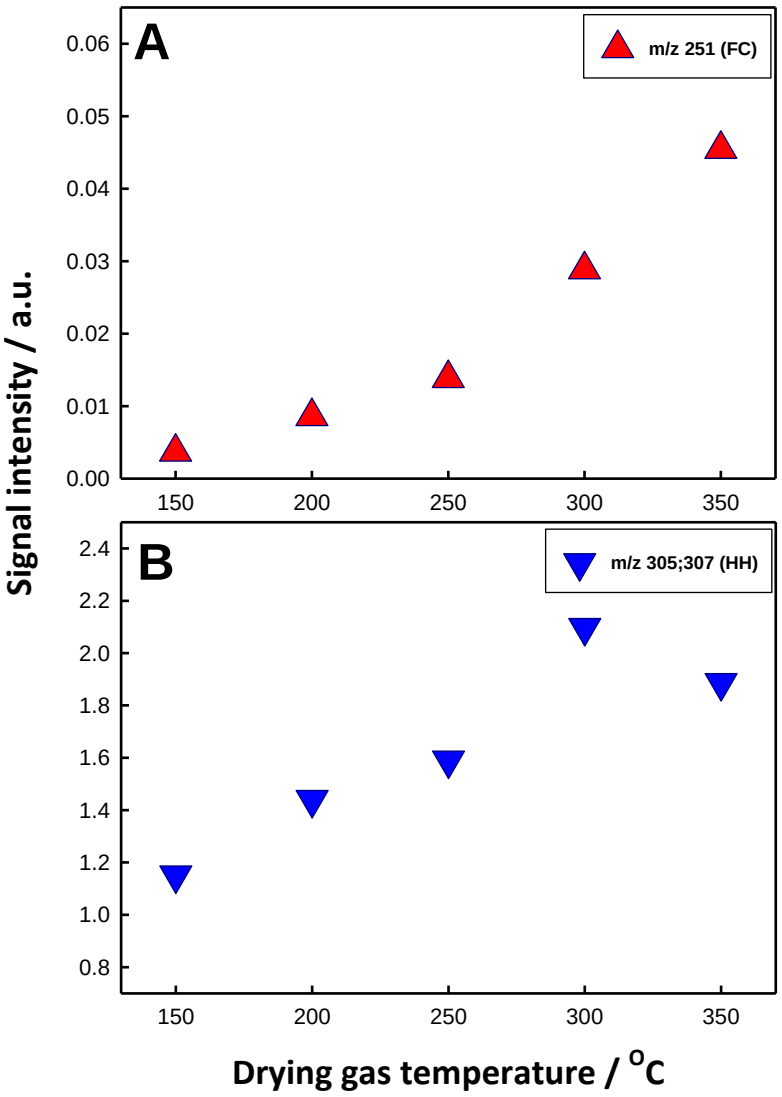

Figure S4 – Mass spectral signal intensities. **A:** m/z 251 (FC). **B:** 305;307 (HH) from [1 mM β-C + 0.2 mM NaCl] in x_w = 0.42 W:AN solutions microjet exposed to O_3(g) [$E(O_3)$ = 9.4 x 10^{10} molecules cm^{-3} s] as a function of drying gas temperature. Note that FC signals steadily increase with temperature, whereas HH signals increase with temperature to a maximum at 300 °C, and decrease afterwards, possibly due to partial thermal decomposition in the heated capillary.

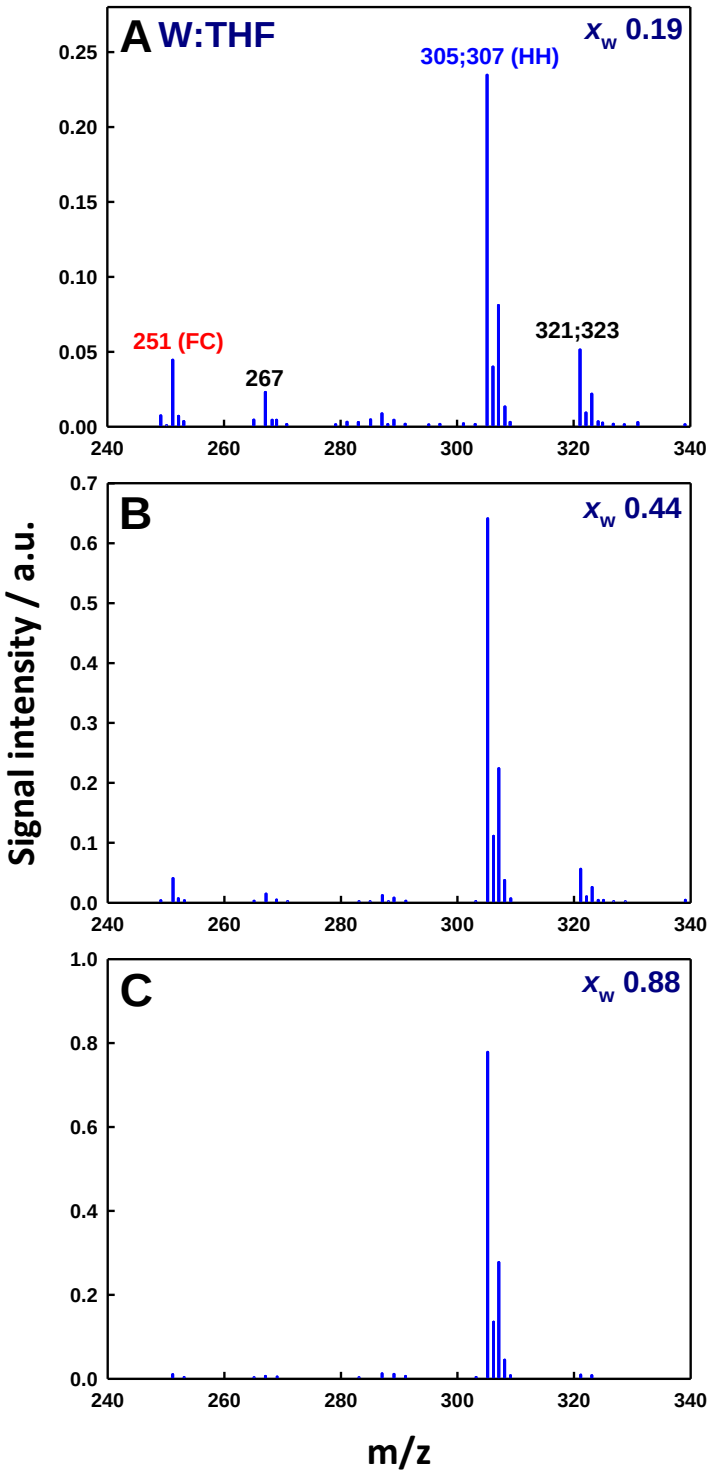

Figure S5 – Negative ion online mass spectra of the interfacial layers of (1 mM β-C + 0.2 mM NaCl) in W:THF liquid microjets exposed to O_3(g), $E(O_3)$ = 3.4 x 10^{10} molecules cm^{-3} s. Molar fractions of water in bulk W:THF mixtures. **A:** x_w = 0.19. **B:** x_w = 0.44. **C:** x_w = 0.88.

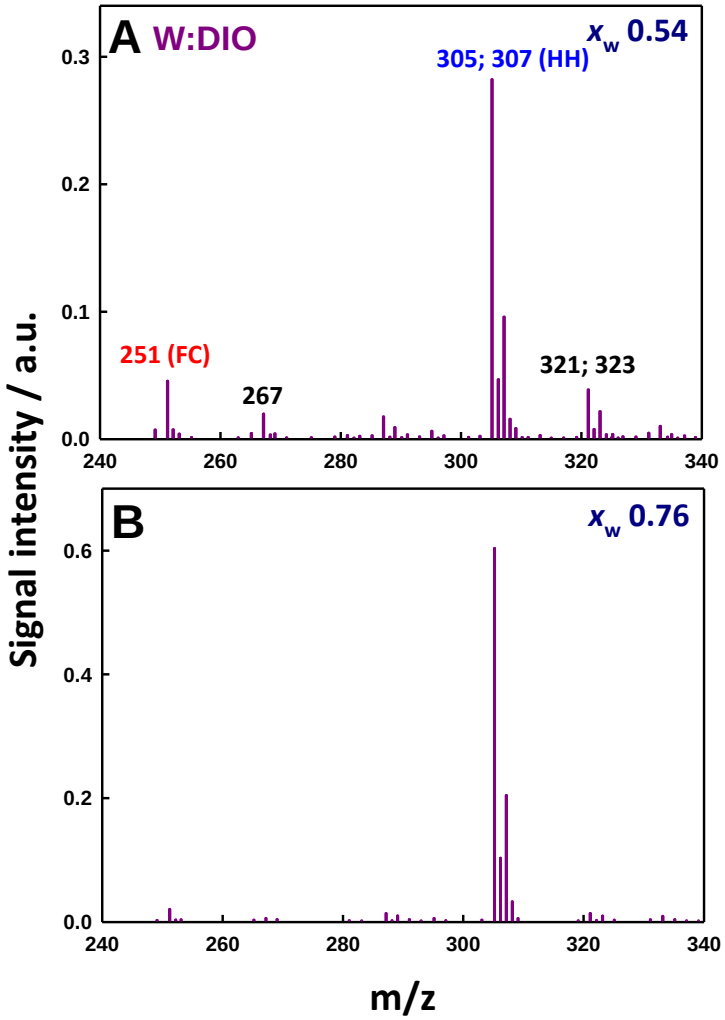

Figure S6 – Negative ion online mass spectra of the interfacial layers of (1 mM β-C + 0.2 mM NaCl) in W:DIO liquid microjets exposed to O_3(g), $E(O_3)$ = 3.9 x 10^{10} molecules cm^{-3} s. Molar fractions of water in bulk W:DIO mixtures. **A:** x_w = 0.54. **B:** x_w = 0.76.

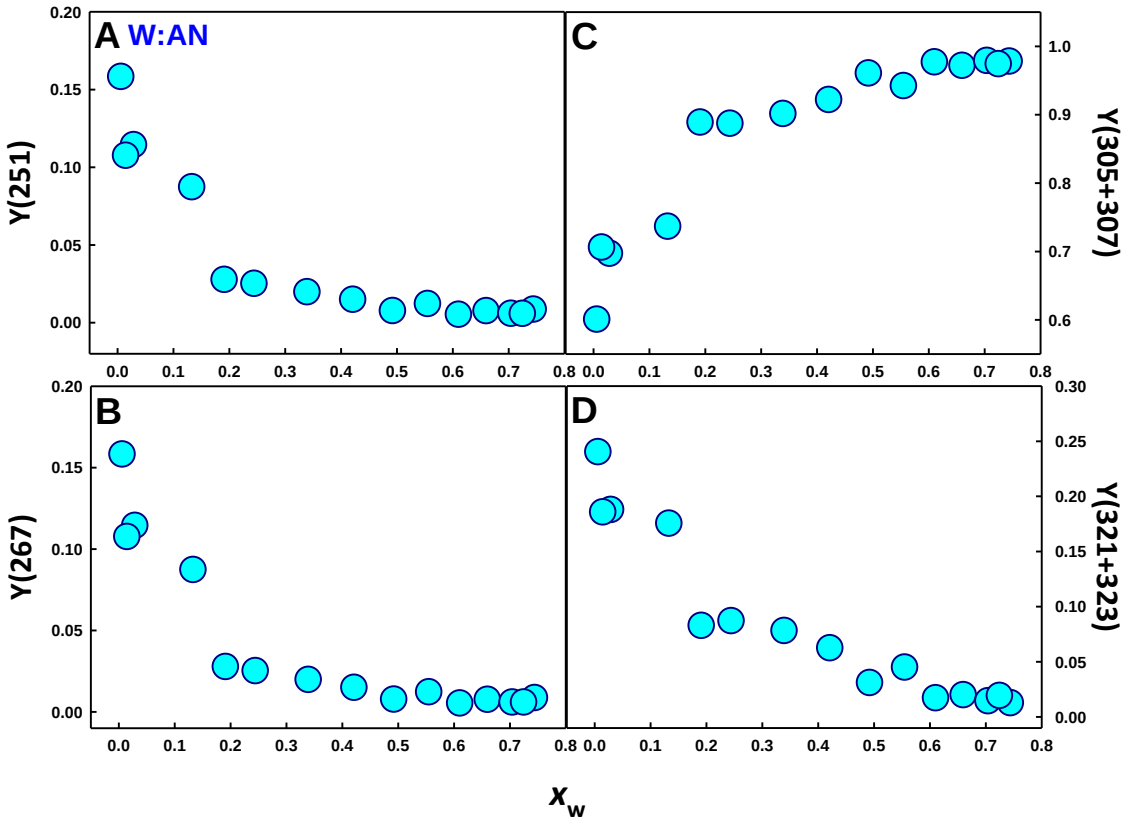

Figure S7 – Product yields $Y(P_i)$ (from equation SE3, below) as functions of molar fraction of bulk water x_w from experiments on [1 mM β-caryophyllene + 0.2 mM NaCl] in W:AN liquid microjets exposed to $E(O_3(g)$, molecules cm^{-3} s) = $(0.9 \pm 0.1) \times 10^{11}$. (A) m/z 251, (B) m/z 267, (C) m/z 305+307, and (D) m/z 321+323. Product yields $Y(P_i)$, defined as: $Y(P_i) = I_{Pi} / \Sigma I_{Pj}$ (SE3), where I_{Pi} is the mass signal intensity of product P_i, as functions of x_w at constant $O_3(g)$ exposure.

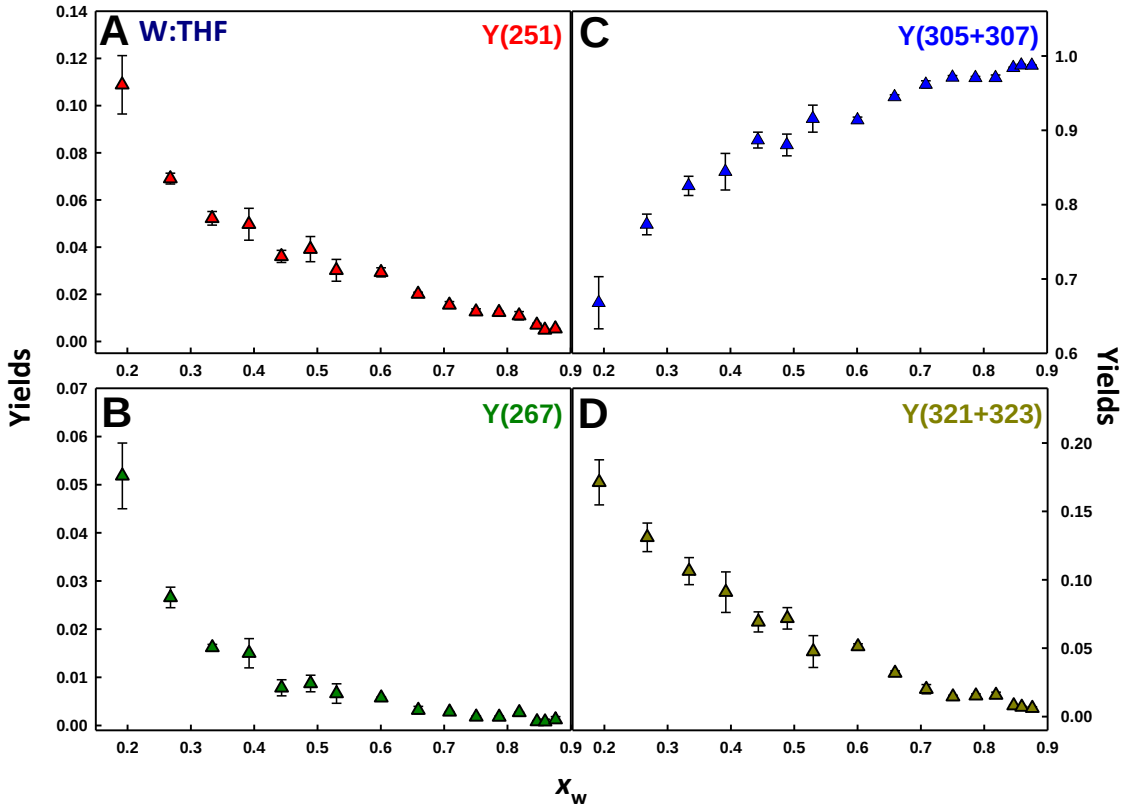

Figure S8 – Product yields Y(P_i) as functions of molar fraction of bulk water x_w from experiments on [1 mM β-caryophyllene + 0.2 mM NaCl] in W:THF liquid microjets exposed to $E(O_3)$ = (3.7 ± 0.5) x 10^{10} molecules cm^{-3} s. (A) m/z 251, (B) m/z 267, (C) m/z 305+307, and (D) m/z 321+323. Error bars derived from triplicated measurements. See caption to Figure S7.

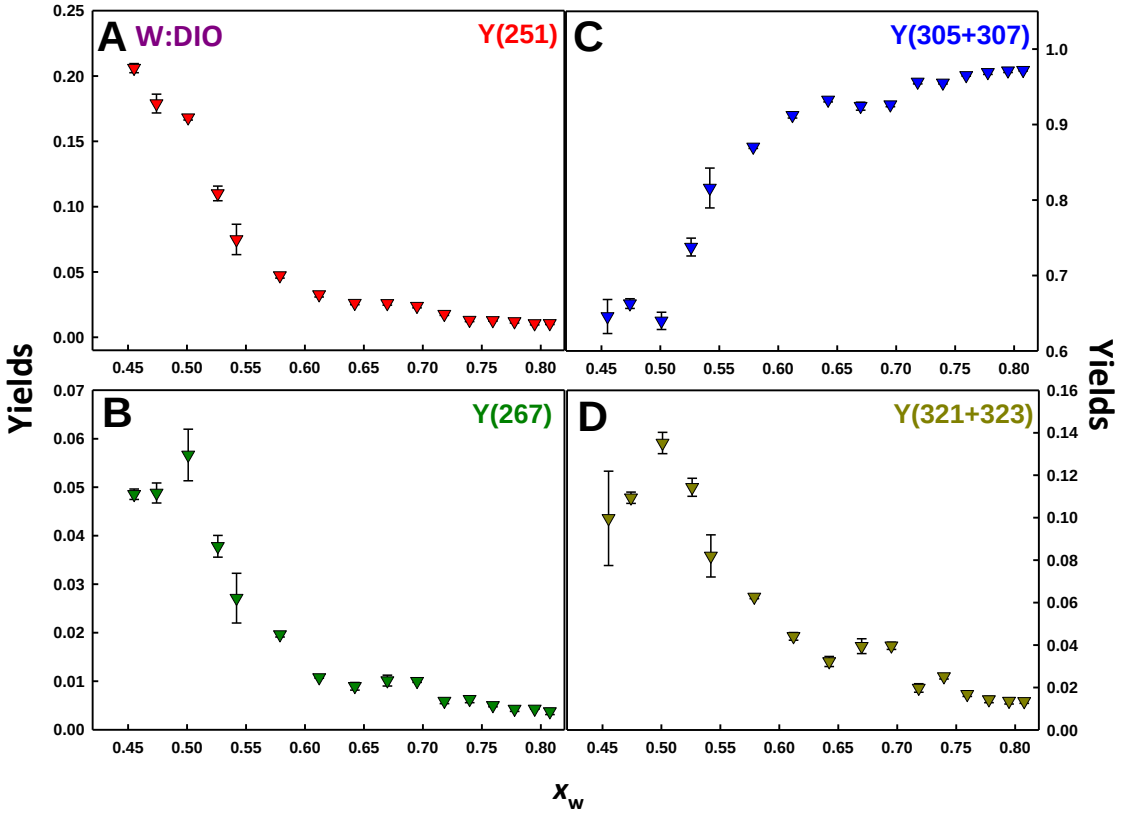

Figure S9 – Product yields Y(P_i) as functions of molar fraction of bulk water x_w from experiments on [1 mM β-caryophyllene + 0.2 mM NaCl] in W:DIO microjets to E = (3.5 ± 0.3) x 10^{10} O_3(g) molecules cm^{-3} s^{-1}. (A) m/z 251, (B) m/z 267, (C) m/z 305+307, and (D) m/z 321+323. Error bars are derived from triplicated measurements. See caption to Figure S7.

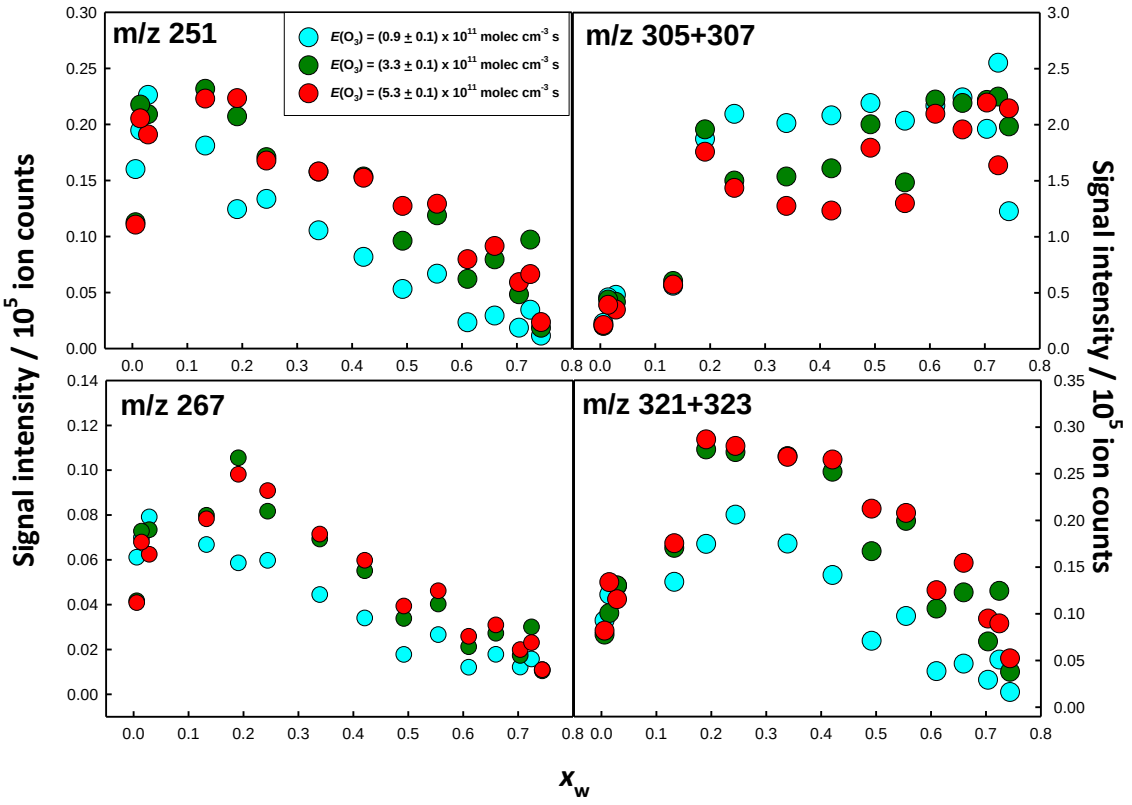

Figure S10 – Absolute signal intensity of m/z 251, 267, 305+307, and 321+323 as a function of molar fraction of bulk water x_w from experiments on [1 mM β-caryophyllene + 0.2 mM NaCl] in W:AN liquid microjets exposed to $E(O_3(g)$, molecules cm^{-3} s) = (0.9 ± 0.1) × 10^{11} (cyan), (3.3 ± 0.1) × 10^{11} (green), (5.3 ± 0.1) × 10^{11} (red), respectively.

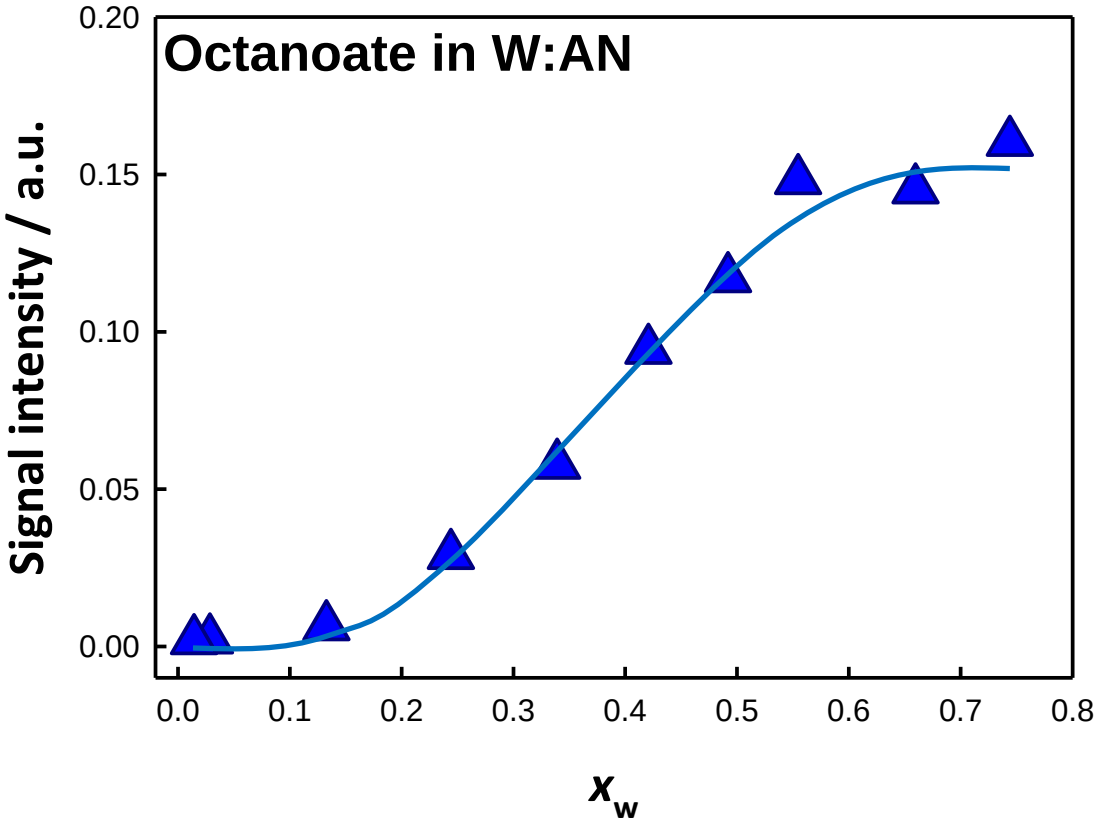

Figure S11 – Octanoate m/z 143 mass spectral signal intensity as a function of the molar fraction of water, x_w, from 5 μM octanoic acid in W:AN microjets. Line is visual guide.

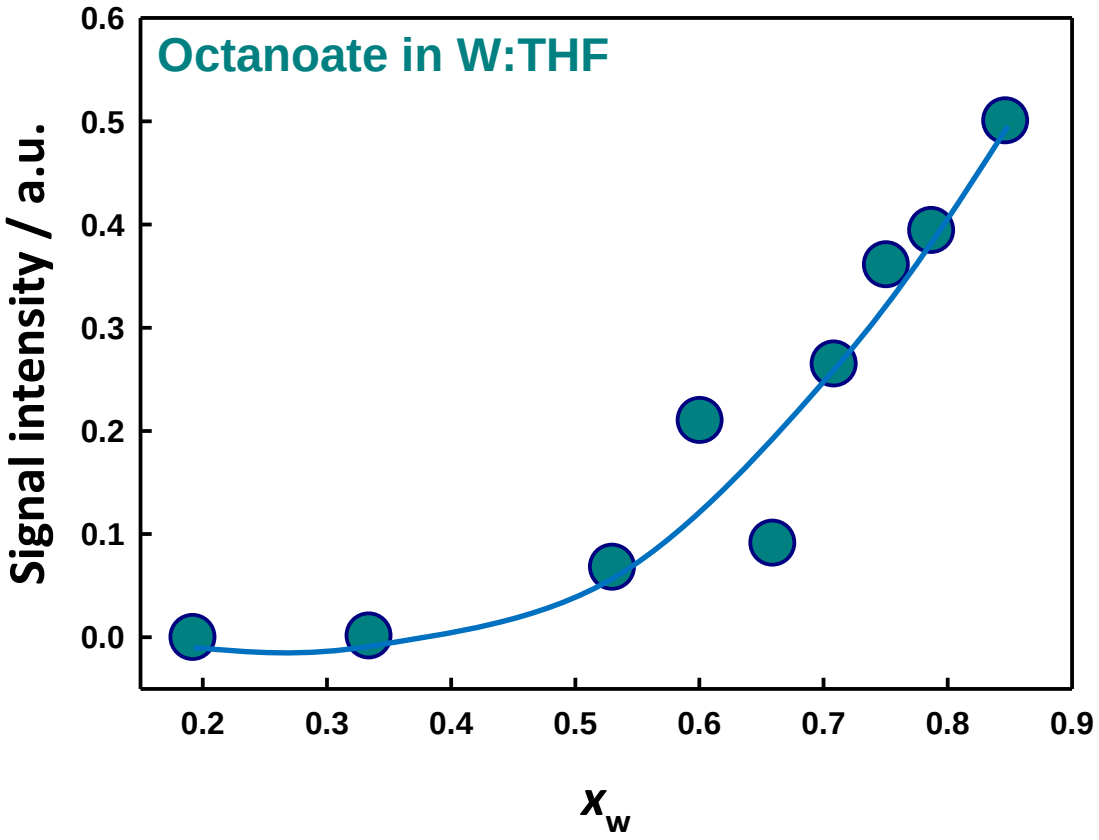

Figure S12 – Octanoate m/z 143 mass spectral signal intensity as a function of the molar fraction of water, x_w, from 5 μM octanoic acid in W:THF microjets. Line is visual guide.

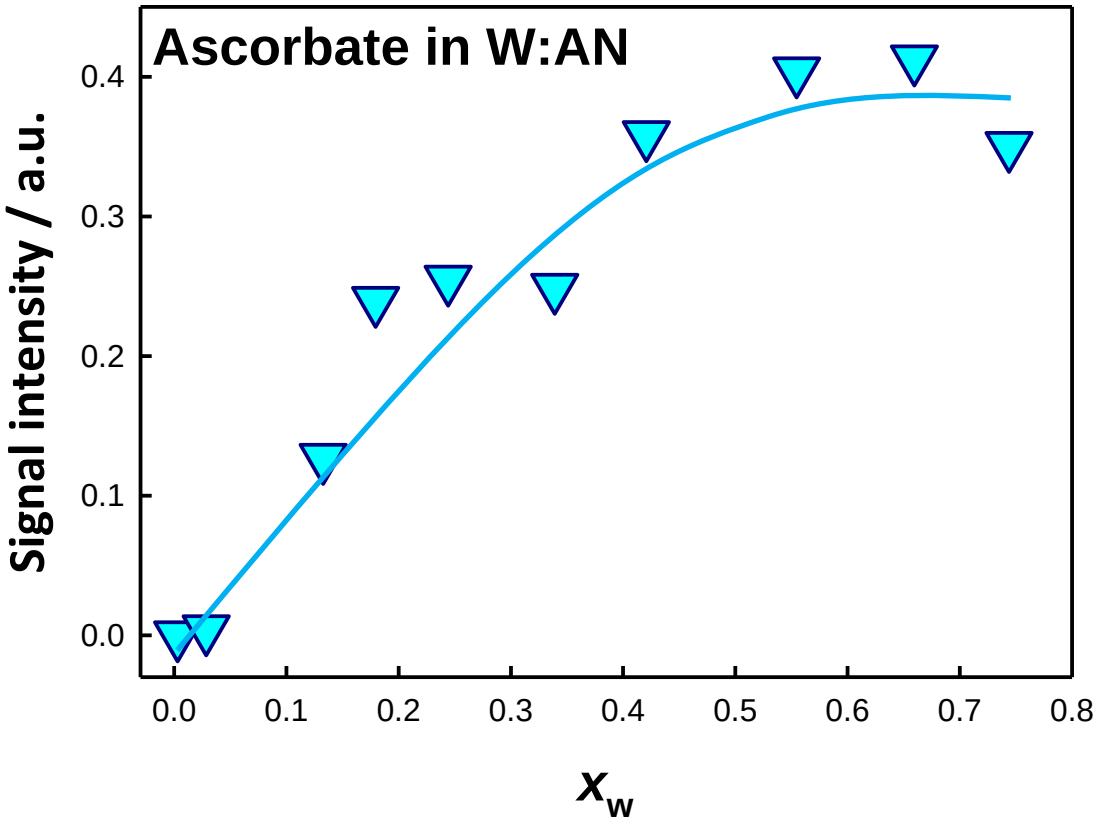

Figure S13 – Ascorbate m/z 175 mass spectral signal intensity as a function of the molar fraction of water, x_w, from 10 μM ascorbic acid in W:AN microjets. Line is visual guide.

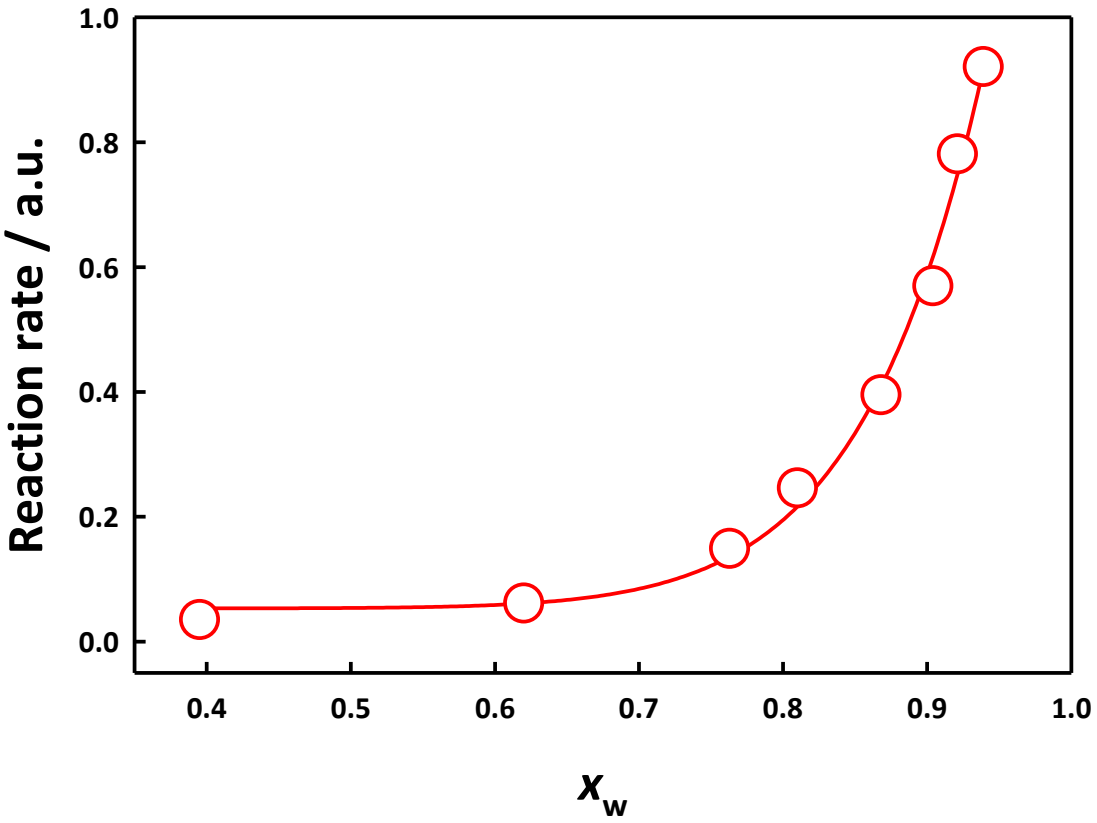

Figure S14 – Reaction rates of tert-butyl chloride relative to the value in pure water as a function of the molar fraction of water x_w in W:AN mixtures. Taken from Wakisaka et al.[2]

1. H. Mishra, S. Enami, R. J. Nielsen, M. R. Hoffmann, W. A. Goddard and A. J. Colussi, Proc. Natl. Acad. Sci. U .S. A. **109** (26), 10228-10232 (2012).

2. A. Wakisaka, Y. Shimizu, N. Nishi, K. Tokumaru and H. Sakuragi, J. Chem. Soc. Faraday Trans. **88** (8), 1129-1135 (1992).